Piperazine ferulate attenuates high glucose-induced mesangial cell injury via the regulation of p66^{Shc}

YONG-YU YANG[1,2], RONG-RONG DENG[3], ZHUO CHEN[4], LIANG-YUAN YAO[2,5], XI-DING YANG[1] and DA-XIONG XIANG[1,2]

[1]Department of Pharmacy, [2]Hunan Provincial Engineering Research Central of Translational Medical and Innovative Drug, The Second Xiangya Hospital of Central South University, Changsha, Hunan 410011; [3]School of Traditional Chinese Medicine, Guangdong Pharmaceutical University, Guangzhou, Guangdong 510006; [4]Department of Geriatrics, The Third Xiangya Hospital of Central South University, Changsha, Hunan 410013; [5]Hunan Qianjin Xiangjiang Pharmaceutical Industry Co., Ltd., Zhuzhou, Hunan 412000, P.R. China

Received September 21, 2020; Accepted February 22, 2021

DOI: 10.3892/mmr.2021.12013

Abstract. Diabetic nephropathy (DN) is a severe microvascular complication of diabetes. Hyperglycemia-induced glomerular mesangial cells injury is associated with microvascular damage, which is an important step in the development of DN. Piperazine ferulate (PF) has been reported to exert protective effects against the progression of DN. However, whether PF prevents high glucose (HG)-induced mesangial cell injury remains unknown. The aim of the present study was to investigate the effects of PF on HG-induced mesangial cell injury and to elucidate the underlying mechanisms. Protein and mRNA expression levels were determined via western blot analysis and reverse transcription-quantitative PCR, respectively. IL-6 and TNF-α levels were measured using ELISA. Reactive oxygen species levels and NF-κB p65 nuclear translation were determined via immunofluorescence analysis. Apoptosis was assessed by measuring lactate dehydrogenase (LDH) release, as well as using MTT and flow cytometric assays. The mitochondrial membrane potential of mesangial cells was determined using the JC-1 kit. The results revealed that LDH release were increased; however, cell viability and mitochondrial membrane potential were decreased in the HG group compared with the control group. These changes were inhibited after the mesangial cells were treated with PF. Moreover, PF significantly inhibited the HG-induced production of inflammatory cytokines and the activation of NF-κB in mesangial cells. PF also attenuated the HG-induced upregulation of the expression levels of fibronectin and collagen 4A1. Furthermore, the overexpression of p66$^{Src\ homology/collagen\ (Shc)}$ abolished the protective effect of PF on HG-induced mesangial cell injury. *In vivo* experiments revealed that PF inhibited the activation of inflammatory signaling pathways, glomerular cell apoptosis and mesangial matrix expansion in diabetic mice. Collectively, the present findings demonstrated that PF attenuated HG-induced mesangial cells injury by inhibiting p66^{Shc}.

Correspondence to: Mrs. Xi-Ding Yang or Professor Da-Xiong Xiang, Department of Pharmacy, The Second Xiangya Hospital of Central South University, 139 Renminzhong Road, Changsha, Hunan 410011, P.R. China
E-mail: xidingyang@csu.edu.cn
E-mail: xiangdaxiong@csu.edu.cn

Key words: piperazine ferulate, inflammatory cytokine, diabetic nephropathy, apoptosis, p66 $^{Src\ homology/collagen}$, mesangial cells

Introduction

Diabetic nephropathy (DN) is a serious complication of diabetes, and is the most common cause of end-stage renal disease in developed countries (1). It was estimated that the total number of individuals with diabetic mellitus worldwide will reach 693 million in 2045 (2). In addition, ~20-40% of all diabetic patients will develop DN (3). High glucose (HG) and HG-induced oxidative stress, inflammation and hemodynamic changes serve an important role in glomerular injury, which is a hallmark of DN (4,5). In diabetes, HG affects all cells in the kidneys, including endothelial cells, renal tubular epithelial cells, renal interstitial fibroblasts, podocytes and mesangial cells (6-8). Mesangial cells are specialized smooth muscle cells between capillary loops of the glomerular capillary, and are involved in the physiological and pathological changes of glomera function (9). Mesangial cell injury, characterized by an increase in apoptosis, excessive inflammatory cytokine production and extracellular matrix synthesis, is a basic pathological change of DN (7,9). Clinical, animal and *in vitro* studies have revealed that HG can induce mesangial cell apoptosis, which aggravates the pathological process of DN (10,11). The hyperglycemia-induced excessive generation of reactive oxygen species (ROS) has been recognized as one of the causes for DN (10-12); however, the precise mechanisms involved are yet to be fully elucidated.

p66$^{Src\ homology/collagen\ (Shc)}$ is a member of the ShcA protein family and acts as a response protein that modulates the response to oxidative stress (13). p66^{Shc} is mainly located in the cytoplasm; however, when it is activated under stress conditions, it enters the mitochondria and acts with cytochrome *c* to

produce ROS (14). Moreover, $p66^{Shc}$ is known to serve a major role in various kidney diseases, such as drug-induced acute kidney injury (15), hypertension-induced nephropathy (16) and DN (17). $p66^{Shc}$ knockout has been reported to protect mesangial cells from HG-induced apoptosis (17), as well as protect against renal tubular injury (18) and injury to podocytes (19). Therefore, treatments targeted at $p66^{Shc}$ may be beneficial for DN.

Piperazine ferulate (PF; $C_4H_{10}N_2{\cdot}2C_{10}H_{10}O_4$; 474.51 g/mol; Fig. 1A), a compound synthesized by ferulic acid and piperazine, is used in the treatment of various types of kidney disease including DN, nephritis (20) and immunoglobulin (Ig) A nephropathy (21) in China. Previous research has revealed that PF reduces the levels of blood urea nitrogen and serum creatinine in rats subjected to 5/6 nephrectomy (22) and exerts anti-hypertensive effects via the activation of endothelial nitric oxide synthase (eNOS) (23). Another previous study reported that PF administration can restore the HG-induced expression of eNOS in glomerular endothelial cells and delay the development of DN (24). However, it remains unknown as to whether PF restores mesangial cell injury under hyperglycemic conditions by inhibiting $p66^{Shc}$.

In the present study, the effects of PF on the mesangial cell injury under hyperglycemic conditions were investigated.

Materials and methods

Materials. The lactate dehydrogenase (LDH) activity kit, TRIzol® reagent, BCA protein assay kit, primary antibody dilution buffer, RIPA, PMSF, dihydroethidium and the BeyoECL plus kit were obtained from Beyotime Institute of Biotechnology. The IL-6 ELISA kit (cat. no. EK0411) and TNF-α ELISA kit (cat. no. EK0527) were purchased from Boster Biological Technology. SYBR® Premix Ex Taq™ and the PrimeScript reverse transcription reagent kit were obtained from Takara Biotechnology Co., Ltd. The Annexin V-FITC kit was purchased from BD Biosciences. MTT assay and the JC-1 probe were purchased from Beijing Solarbio Science & Technology Co., Ltd. PF was obtained from Hunan QianJinXiangJiang Pharmaceutical Industry Co., Ltd. D-glucose, D-mannitol, 5% bovine serum albumin (BSA) blocking buffer and the Masson's Trichrome stain kit (cat. no. G1340) were purchased from Beijing Solarbio Science & Technology Co., Ltd. All antibodies used for western blotting are detailed in Table I.

Animal experiment. Male C57BL/6J mice (weight, 18-22 g; age, 8 weeks) were purchased from the Experimental Animal Center of Silaikejingda. Mice were kept under a 12-h light-dark cycle with a controlled temperature (24±1˚C) and humidity (50±10%), and allowed free to access to food and water. All experimental protocols were approved by the Ethics Committee of Animal Experiments of the Central South University, and were performed in accordance with the Guidelines for the Care and Use of Laboratory Animals.

A total of 45 mice were randomly divided into three groups (n=15 mice per group) as follows: A control group, a model group (DN) and the model + PF group (DN + PF group). Diabetic model mice were established according to a previously described protocol (24). PF was dissolved in 0.5% sodium carboxymethyl cellulose (CMC-Na). DN + PF group mice were treated intraperitoneally with PF (100 mg/kg) once daily for 12 consecutive weeks. Mice in the control and DN groups were administered the same amount of CMC-Na (0.5%). Finally, the mice were anaesthetized with sodium pentobarbital (50 mg/kg body weight) and sacrificed by exsanguination. The kidney tissue was collected for histopathological analysis.

Immunohistochemistry analysis. Kidney tissue was fixed with 4% paraformaldehyde overnight at 4˚C, embedded in paraffin blocks and cut into 5-μm-thick sections. The sections were dewaxed in xylene at room temperature, rehydrated in a descending series of ethanol (100, 95, 80 and 70%), and washed with distilled water at room temperature, followed by blocking with 3% hydrogen peroxidase at room temperature for 10 min, and blocking with 5% BSA for 30 min at 37˚C. The sections were incubated with fibronectin (1:200) and collagen 4A1 (Boster Biological Technology; cat. no. BA2174; 1:200) overnight at 4˚C, followed by incubation with the HRP-conjugated goat anti-rabbit (Boster Biological Technology; cat. no. BA1054; 1:5,000) for 1 h at room temperature. Subsequently, the sections were incubated with the HRP substrate diaminobenzadine for color development and stained with hematoxylin (0.5%) for 1 min at room temperature. All stained sections were evaluated using conventional light microscopy (magnification, x400).

Masson's trichrome staining. Masson's trichrome staining was performed using the Masson's Trichrome staining kit according to the manufacturer's instructions. Briefly, kidney tissue was fixed with 4% paraformaldehyde overnight at 4˚C, embedded in paraffin blocks and cut into 5-μm thick sections. The sections were dewaxed with xylene at room temperature and then rehydrated with gradient ethanol (100, 95, 80 and 50%). After washing with distilled water, sections were incubated with 0.5% Weigert's iron hematoxylin at room temperature for 10 min. After rinsing in distilled water, the sections were stained with 1% hydrochloric acid-alcohol at room temperature for 10 sec, and then stained with 0.7% Ponceau 2R-0.3% acid fuchsin solution at room temperature for 10 min, followed by staining with 1% phosphomolybdic acid solution for 2 min and 2% aniline blue for 2 min at room temperature. Slides were then dehydrated in graded ethanol (30, 50, 70, 95 and 100%) and sealed with neutral gum. The images were captured using a light microscope (magnification, x400).

Cell culture and treatment. Mouse mesangial cells (SV-40 MES-13 cells) were purchased from the China Infrastructure of Cell Line Resource, and cultured in DMEM (HyClone; Cyclone) containing 5% FBS (HyClone; Cytiva) at 37˚C in a humidified incubator with 5% CO_2. To examine the effects of HG on the cell viability, mouse mesangial cells were treated with various concentrations of HG (20, 25, 30 and 35 mM) or mannitol (24.5 mM D-mannitol + 5.5 mM glucose) at 37˚C for 24 h. D-mannitol was used to as an osmotic control for the HG. MTT method was used to evaluate the cell viability.

Cell viability and apoptosis assay. The viability of mouse mesangial cells was evaluated using an MTT assay. Cells were plated in 96-well plates at a density of $1.0x10^5$ cells per well and treated with HG (30 mM) with or without PF (25, 50, 100 and 200 μM) at 37˚C for 24 h. MTT solution (5 mg/ml)

was added to each well, and incubated with the cells at 37˚C for 4 h. Following incubation, 150 μl DMSO was added to each well. The optical density (OD) value was measured using a microplate reader at a wavelength of 450 nm.

The level of LDH released in the cell culture supernatant was detected using the LDH cytotoxicity assay detection kit. Briefly, the cell culture supernatant was obtained following centrifugation at 1,000 x g for 10 min at 4˚C. The supernatant was harvested, and the level of LDH was determined following the manufacturer's instructions of the kit.

Overexpression plasmids. A mouse p66^{Shc} expression plasmid (pcDNA-p66^{Shc}) was constructed by Hunan Fenghui Biotechnology Co., Ltd. Mesangial cells grown in 24-well plates were transfected with the p66^{Shc} overexpression plasmid (pcDNA3.1-p66^{Shc}; 1 or 2 ng/μl) or vector (pcDNA3.1; 2 ng/μl) using Lipofectamine® 3000 reagent (Invitrogen; Thermo Fisher Scientific, Inc.) at 37˚C for 24 h. Mesangial cells were treated with HG (30 mM) in the presence or absence of 100 μM PF at 37˚C for 24 h.

Western blot analysis. Protein expression levels were determined via western blot analysis. Cells or kidney tissue lysates were prepared with RIPA lysis solution containing 10% PMSF. The protein concentration was determined using a BCA protein assay kit and each protein was then denatured at 95˚C for 5 min. Protein samples (35 μg each) were separated by SDS-PAGE on 10% gels and transferred onto a PVDF membrane (EMD Millipore). After blocking with 5% skim milk in TBS containing 0.1% Tween-20 at room temperature for 1 h, the membrane was incubated with primary antibodies against p66^{Shc}, p-P66^{Shc}, caspase-3, p-IKKα/β (Ser176), IKKα/β, Bcl2, Bax, fibronectin, IκBα, p-NF-κB p65 (S536) and β-actin overnight at 4˚C. Antibodies were diluted with primary antibody dilution buffer (as indicated in Table I). Subsequently, the membrane was incubated with HRP-conjugated goat anti-rabbit (Boster Biological Technology; cat. no. BA1054; 1:5,000), HRP-conjugated goat anti-mouse (Boster Biological Technology; cat. no. BA1050; 1:5,000) or HRP-conjugated rabbit anti-goat secondary antibodies (Boster Biological Technology; cat. no. BA1060; 1:5,000). Blots were visualized by the BeyoECL Plus kit, and were captured using an Amersham Imager 600 (Amersham; Cytiva) and semi-quantified using ImageJ 1.37c software (National Institute of Health). The protein level was normalized to that of β-actin.

RNA preparation and reverse transcription-quantitative PCR (RT-qPCR). Total RNA was extracted from the treated cells or kidney tissue using TRIzol according to the manufacturer's instructions. Total RNA (400 ng) was reverse transcribed to cDNA using the PrimeScript RT reagent kit at 37˚C for 15 min and 85˚C for 15 sec. qPCR was performed using SYBR-Green dye I and the LightCycler96® (Roche Diagnostics GmbH). The sequences of the RT-qPCR primers were as follows: Fibronectin forward, 5'-AGGCTGGATGATGGTGGACT-3' and reverse, 5'-TGCTCCACGTGTCTCCAATC-3'; collagen 4A1 forward, 5'-GGCATTGTGGAGTGTCAACC-3' and reverse, 5'-ACAGGCAAGGCAGCTCTCTC-3'; and β-actin forward, 5'-ACTGCTCTGGCTCCTAGCAC-3' and reverse, 5'-ACATCTGCTGGAAGGTGGAC-3'. The thermal profile settings were as follows: Initial denaturation at 95˚C for 30 sec, followed by 40 cycles of denaturation at 95˚C for 5 sec and annealing at 60˚C for 31 sec. The relative mRNA expression levels were normalized to the expression of β-actin and calculated using the $2^{-\Delta\Delta Cq}$ method (25).

Determination of inflammatory cytokine levels. The levels of IL-6 and TNF-α in the cell supernatants were measured using ELISA kits. Briefly, the cell culture supernatant was obtained following centrifugation at 1,000 x g for 10 min at 4˚C and the levels of IL-6 and TNF-α were determined according to the manufacturers' instructions. All samples were measured in triplicate.

ROS measurement. Intracellular ROS levels were measured using dihydroethidium. Following treatment, mesangial cells were washed with PBS, and then incubated in serum-free DMEM with 5 μM dihydroethidium for 30 min at 37˚C. The fluorescence of ethidium was detected using a fluorescence microscope (Carl Zeiss AG) at an excitation wavelength of 535 nm and emission wavelength of 610 nm.

Immunofluorescence analysis. The cells were fixed in 4% paraformaldehyde for 15 min at room temperature, and then washed three times with 0.01 M PBS for 5 min each. Following incubation with 0.1% Triton X-100 at room temperature for 10 min, the cells were blocked in PBS-B solution and incubated with specific anti-NF-κB p65 primary antibody at 4˚C overnight. The cells were then incubated with Cy3 antibody (Beyotime Institute of Biotechnology; cat. no. A0516; 1:500) for at room temperature for 1 h and the nuclei were stained with DAPI at room temperature for 10 min. Images were captured using a fluorescence microscope (magnification, x400).

JC-1 staining. The mitochondrial membrane potential of the mesangial cells was determined using a JC-1 kit according to the manufacturer's instructions. This method is based on the ability of JC-1 to form red fluorescent in normal mitochondria (aggregates state of JC-1). The loss of mitochondrial membrane potential generates the reduction of red fluorescence and a concomitant increase in green fluorescence (monomeric state of JC-1) (26). The cells were washed with PBS three times and incubated in JC-1 dye at 37˚C for 30 min. Images were captured using a fluorescence microscope at an excitation/emission wavelength of 485/590 nm (magnification, x400).

TUNEL assay. TUNEL staining was used to label apoptotic cells in the glomerulus, according the manufacturer's protocol. Briefly, the kidney tissue was fixed with 4% paraformaldehyde at 4˚C overnight, and then dehydrated in an ascending series of ethanol (70, 80, 90, 95 and 100%), embedded in paraffin and sectioned (5-μm thickness). Subsequently, the sections were deparaffinized with xylene at room temperature, rehydrated with a descending series of ethanol (100, 90 and 70%), and then incubated with proteinase K for 30 min at room temperature. After washing with PBS, the sections were incubated with TUNEL reaction mixture (Beyotime Institute of Biotechnology; cat. no. C1089) at 37˚C for 1 h. After washing with PBS thrice, the sections were stained with DAPI (5 μg/ml) at room temperature for 5 min, prior to addition of the antifade mounting medium (Beyotime Institute of Biotechnology;

Table I. Specific details of the antibodies used in western blot analysis.

Target	Supplier (cat. no.)	Clone	Species	Dilution
$p66^{Shc}$	Novus Biological, LLC (NBP2-20352)	Polyclonal Ab.	Rabbit	1:500
p-$p66^{Shc}$ (Ser36)	Abcam (ab54518)	Monoclonal Ab.	Mouse	1:1,000
IκBα	Abcam (ab32518)	Monoclonal Ab.	Rabbit	1:500
p-NF-κB p65 (S536)	Abcam (ab76302)	Monoclonal Ab.	Rabbit	1:1,000
p-IKKα/β (Ser 176)	Santa Cruz Biotechnology, Inc. (sc-21661)	Polyclonal Ab.	Goat	1:500
IKKα/β	Affinity Biosciences (AF6014)	Polyclonal Ab.	Rabbit	1:300
NF-κB p65	Beyotime Institute of Biotechnology (AF1234)	Monoclonal Ab.	Rabbit	1:500
Caspase-3	Beyotime Institute of Biotechnology (AF0081)	Polyclonal Ab.	Rabbit	1:500
Bcl2	Boster Biological Technology (BA0412)	Polyclonal Ab.	Rabbit	1:300
Fibronectin	Boster Biological Technology (BA1772)	Polyclonal Ab.	Rabbit	1:500
Bax	Boster Biological Technology (A00183)	Polyclonal Ab.	Rabbit	1:500
β-actin	Boster Biological Technology (BM0627)	Monoclonal Ab.	Mouse	1:500

Ab, antibody; p-, phosphorylated; Shc, Src homology/collagen.

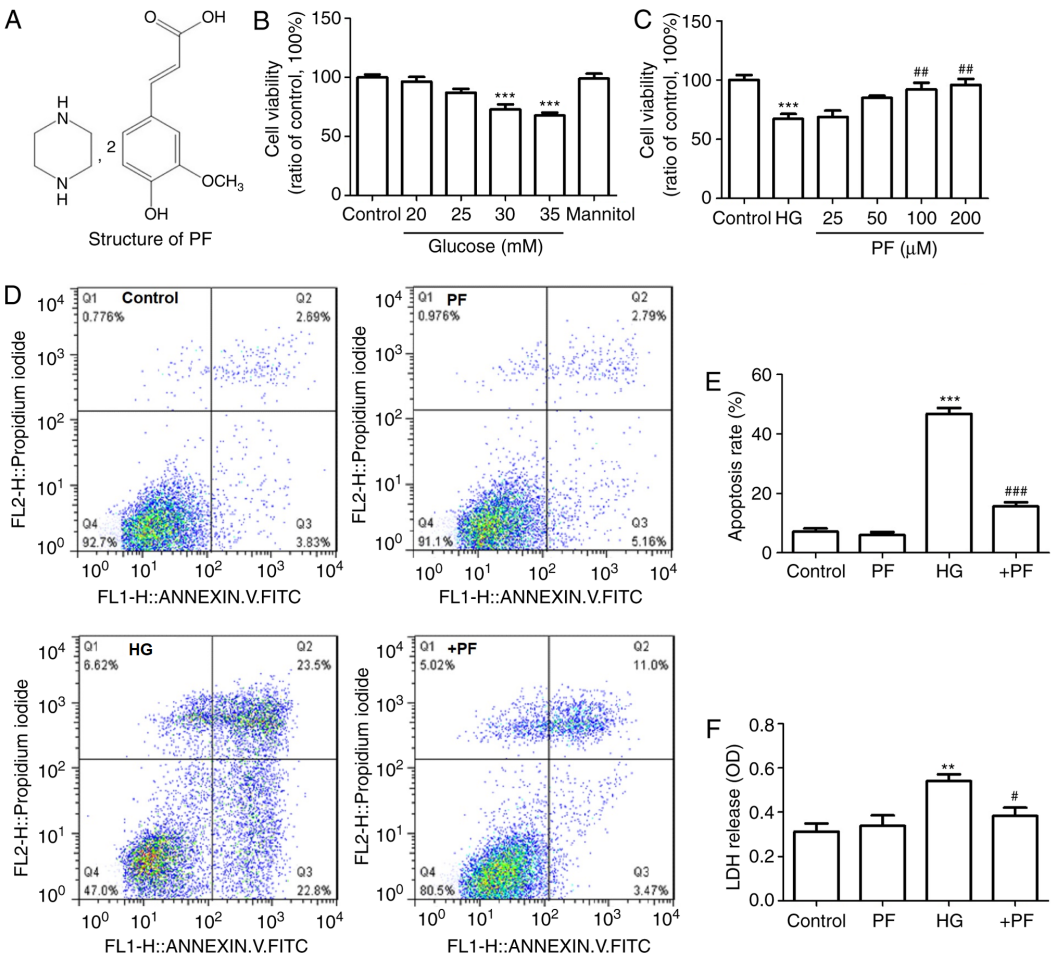

Figure 1. PF prevents the mesangial cell injury induce by HG. (A) Structure of PF. (B) Effect of various concentration of HG on cell viability. (C) Effect of various concentration of PF on HG-induced cell damage (HG, 30 mM). (D) Representative flow cytometric results. (E) Statistical analysis of the flow cytometry data. (F) Level of LDH released in the supernatant of cultured cells. Data are expressed as the mean ± SEM, n=3. **P<0.01, ***P<0.001 vs. control group; $^{\#}$P<0.05, $^{\#\#}$P<0.01, $^{\#\#\#}$P<0.001 vs. HG group. PF, piperazine ferulate; HG, high glucose; OD, optical density; LDH, lactate dehydrogenase; +PF, HG + PF.

cat. no. P0126). Finally, the images were captured using a fluorescence microscope (magnification, x400) in six randomly selected fields of view.

Flow cytometry analysis. Following HG treatment, mesangial cells were collected and washed with PBS three times. A total of 1-5x10^5 cells were suspended in binding buffer, and

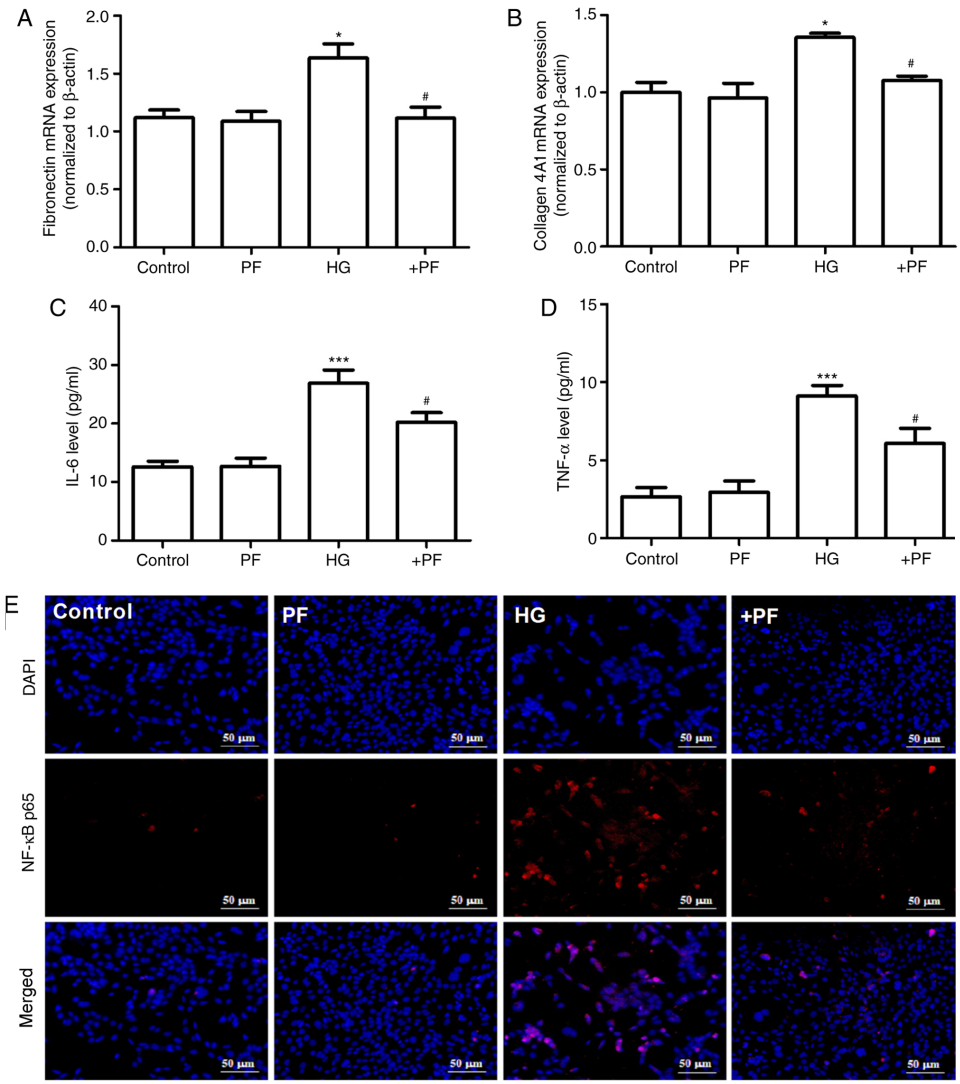

Figure 2. PF attenuates the production of inflammatory cytokines and fibrosis in mesangial cells induced by HG. (A) Fibronectin mRNA expression. (B) Collagen 4A1 mRNA expression. (C) Level of IL-6 in cell culture supernatant. (D) Level of TNF-α in cell culture supernatant. (E) Immunofluorescence image of NF-κB p65; x400 magnification. Data are expressed as the mean ± SEM, n=3. *P<0.05, ***P<0.001 vs. control group; $^{\#}$P<0.05 vs. HG group. PF, piperazine ferulate; HG, high glucose; +PF, HG + PF.

5 μl Annexin V-FITC and 5 μl PI were added. After mixing, the tube was incubated in the dark at room temperature for 15 min. The samples were analyzed using a BD FACSCalibur cell sorting system (BD Biosciences) within 1 h, and data were analyzed using FlowJo 7.6.1 software (FlowJo LLC).

Statistical analysis. Statistical analysis was performed using SPSS software (version 17.0; SPSS, Inc.). One-way ANOVA followed by Tukey's test was performed for multiple groups (≥3) comparisons. Data are presented as the mean ± SEM from ≥3 independent experiments. P<0.05 was considered to indicate a statistically significant difference.

Results

PF inhibits the mesangial cells injury induced by HG. Mouse mesangial cells were treated with various concentrations of HG (20, 25, 30 and 35 mM) to examine the effects of HG on the cell viability. As presented in Fig. 1B, HG (30 or 35 mM) treatment resulted in a significant decrease in cell viability compared with the control group, while mannitol (30 mM) exerted no effect on cell viability.

The effect of various concentrations of PF (25, 50, 100 and 200 μM) on the HG-induced decrease in the viability of mesangial cells was examined. The results demonstrated that pre-incubation of the mesangial cells with PF (100 and 200 μM) caused in an increase in cell viability compared with the HG (30 mM) group (Fig. 1C). The subsequent experiments were performed using 100 μM concentrations of PF.

The results of flow cytometry and LDH release assay revealed that cell apoptosis and LDH release were significantly increased in the HG group, compared with the control group, and these effects were attenuated by incubation with PF (Fig. 1D-F). These results suggested that PF prevented mesangial cell injury induced by HG.

PF attenuates HG-induced inflammatory cytokine and fibrosis in mesangial cells. The effects of PF on the HG-induced inflammatory response and fibrosis in mesangial cells were evaluated. As presented in Fig. 2A and B, compared with the

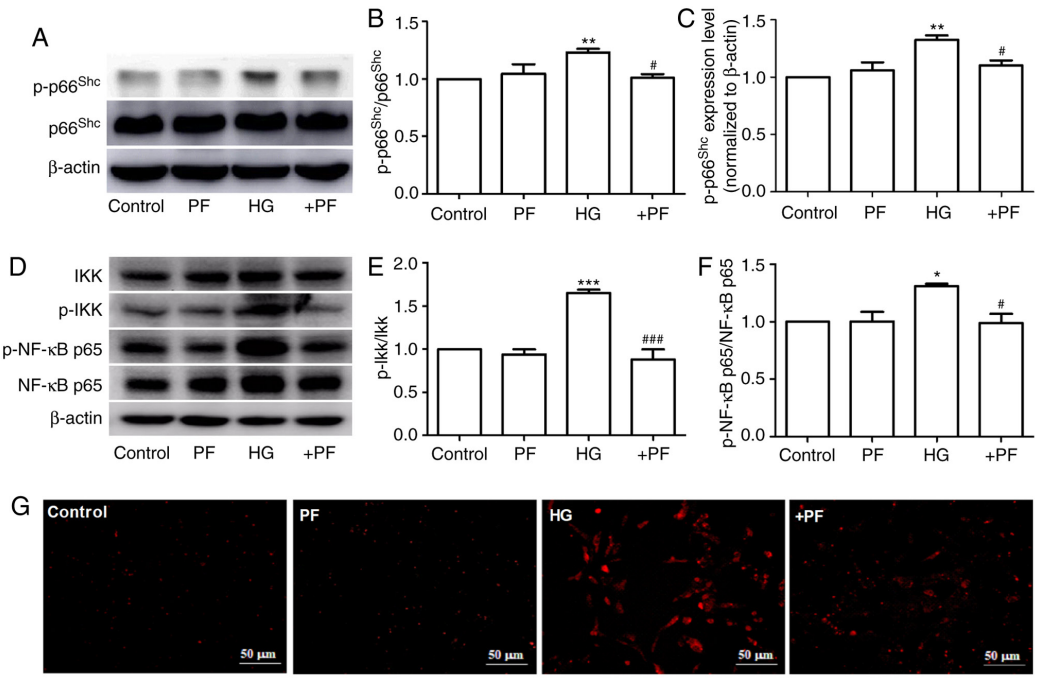

Figure 3. PF inhibits the expression of p-p66^{Shc} in HG-exposed mesangial cells. (A) Western blot analysis of p-p66^{shc} and total p66^{shc}. (B) Densitometric analyses of p-p66^{shc}/p66^{shc} and (C) p-p66^{shc}. (D) Western blot analysis of IKKα/β, p-IKKα/β, NF-κB p65 and p-NF-κB p65. (E) Densitometric analyses of p-IKKα/β/IKKα/β and (F) p-NF-κB p65/NF-κB p65. (G) Fluorescence image of ROS detected using dihydroethidium; x400 magnification. Data are expressed as the mean ± SEM, n=3. *P<0.05, **P<0.01, ***P<0.001 vs. control group; $^{\#}$P<0.05, $^{\#\#\#}$P<0.001 vs. HG group. PF, piperazine ferulate; HG, high glucose; p-, phosphorylated; Shc, Src homology/collagen; +PF, HG + PF.

control group, the mRNA expression levels of fibronectin and collagen 4A1 in mesangial cells were increased following HG treatment, and these changes were mitigated when the mesangial cells were incubated with PF. Likewise, treatment of the mesangial cells with PF significantly reversed the increase in the IL-6 and TNF-α levels in the cell supernatant induced by HG (Fig. 2C and D).

The results of immunofluorescence analysis demonstrated that, compared with the control group, HG induced p65 translocation from the cytoplasm to the nucleus, and PF attenuated this effect in the HG-treated mesangial cells (Fig. 2E). Taken together, these results suggest that PF attenuates the HG-induced production of inflammatory cytokines and fibrosis in mesangial cells.

PF inhibits the expression of p-p66^{Shc} in HG-induced mesangial cells. It has been previously reported that p66^{Shc} is involved in the progression of DN (27), and the phosphorylation of p66^{Shc} at serine 36 serves a key role in p66^{Shc} activation (28). The present study identified that HG induced an increase in p-p66^{Shc} or p-p66^{Shc}/p66^{Shc} protein expression levels in mesangial cells compared with the control group, but had no effect on p66^{Shc} expression. Moreover, co-incubation with PF decreased the HG-induced phosphorylation of p66^{Shc} (Fig. 3A-C). Similarly, treatment of the mesangial cells with PF reversed the increase in the expression levels of p-IKKα/β/IKKα/β and p-NF-κB p65/NF-κB p65 induced by HG (Fig. 3D-F). The result of immunofluorescence analysis demonstrated that PF prevented the HG-induced ROS generation in mesangial cells (Fig. 3G). These results indicate that PF inhibits the HG-induced phosphorylation of p66^{Shc}, IKKα/β and NF-κB p65, as well as ROS generation.

PF regulates HG-induced mesangial cells injury by inhibiting p66^{Shc}. To assess whether p66^{Shc} mediates the protective effects of PF against mesangial cell damage induced by HG, the overexpression of the p66^{Shc} gene was induced using a p66^{Shc} plasmid (Fig. 4A and B). PF treatment attenuated the HG-induced the increased level of IL-6 in the cell culture supernatant, while co-treatment of the mesangial cells with pcDNA-p66^{Shc} abolished the cytoprotective effects of PF (Fig. 4C). PF was demonstrated to attenuate the increase in cleaved caspase-3, p-IKK, Bax and fibronectin expression levels and the decrease in Bcl2 expression in mesangial cells exposed to HG, and co-treatment with pcDNA-p66^{Shc} was able to reverse the protective effects of PF under HG conditions (Fig. 4D-I). Furthermore, PF treatment restored the decrease in the mitochondrial membrane potential of mesangial cells exposed to HG, and the protective effects of PF were abrogated when the mesangial cells were transfected with p66^{Shc} plasmid (Fig. 4J). These data indicated that PF exerted its protective effects via the inhibition of p66^{Shc}.

PF attenuates inflammation and apoptosis in the kidney tissue of diabetic mice. Subsequently, the effects of PF on apoptosis and inflammatory signaling molecules in the kidney tissues of diabetic mice were assessed. As presented in Fig. 5A-D, PF attenuated the HG-induced increase in the protein expression levels of p66^{shc}, p-p66^{shc}, p-p66^{Shc}/p66^{Shc}, p-NF-κB p65/NF-κB p65 and p-IKK/IKK, and restored the loss of IκBα protein expression observed in kidney tissue of diabetic mice. The results of TUNEL assay revealed that PF treatment also caused a notable decrease in glomerular cell apoptosis (Fig. 5E). These results indicated that PF inhibited the activation of inflammatory signals and apoptosis *in vivo*.

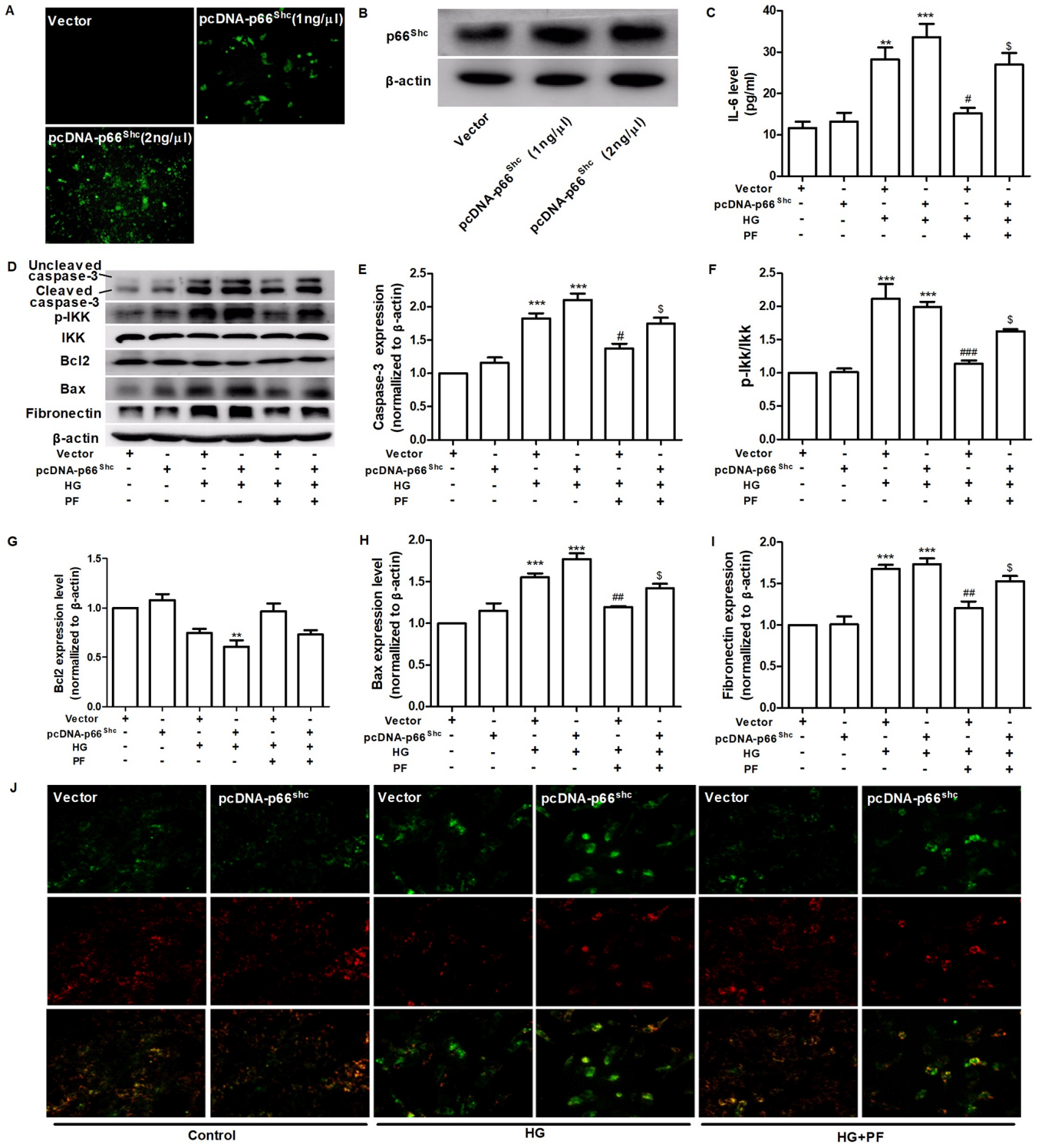

Figure 4. PF regulates HG-induced mesangial cell injury by inhibiting p66^{shc}. (A) Effect of pcDNA-p66^{shc} (1 ng/μl or 2 ng/μl) on the expression of p66^{shc}. (B) Western blot analysis verified the validity of the pcDNA-p66^{Shc}. (C) Level of IL-6 in the cell culture supernatant. (D) Western blot analysis of caspase-3, p-IKKα/β, total IKKα/β, Bcl2, Bax, fibronectin and β-actin. Densitometric analyses of (E) caspase-3, (F) p-IKK/IKK, (G) Bcl2, (H) Bax and (I) fibronectin. (J) Representative image of mesangial cells stained with JC-1 (red for aggregate form of JC-1 and green for monomeric form); x400 magnification. Data are expressed as the mean ± SEM, n=3. **P<0.01, ***P<0.001 vs. vector group; $^{\#}$P<0.05, $^{\#\#}$P<0.01, $^{\#\#\#}$P<0.001 vs. vector + HG group; $^{\$}$P<0.01 vs. vector + HG + PF group. PF, piperazine ferulate; HG, high glucose; vector, empty vector control; p-, phosphorylated; Shc, Src homology/collagen.

PF attenuates mesangial matrix expansion in diabetic mice. The results of RT-qPCR revealed that the mRNA expression levels of collagen 4A1 and fibronectin were increased in the model group when compared with the control group. Furthermore, PF reversed these changes in the mRNA expression levels of collagen 4A1 and fibronectin (Fig. 6A and B). Immunohistochemistry revealed that hyperglycemia increased the expression levels of collagen 4A1 and fibronectin in the glomerulus, and these effects were inhibited by PF (Fig. 6C-E). Masson's trichrome staining

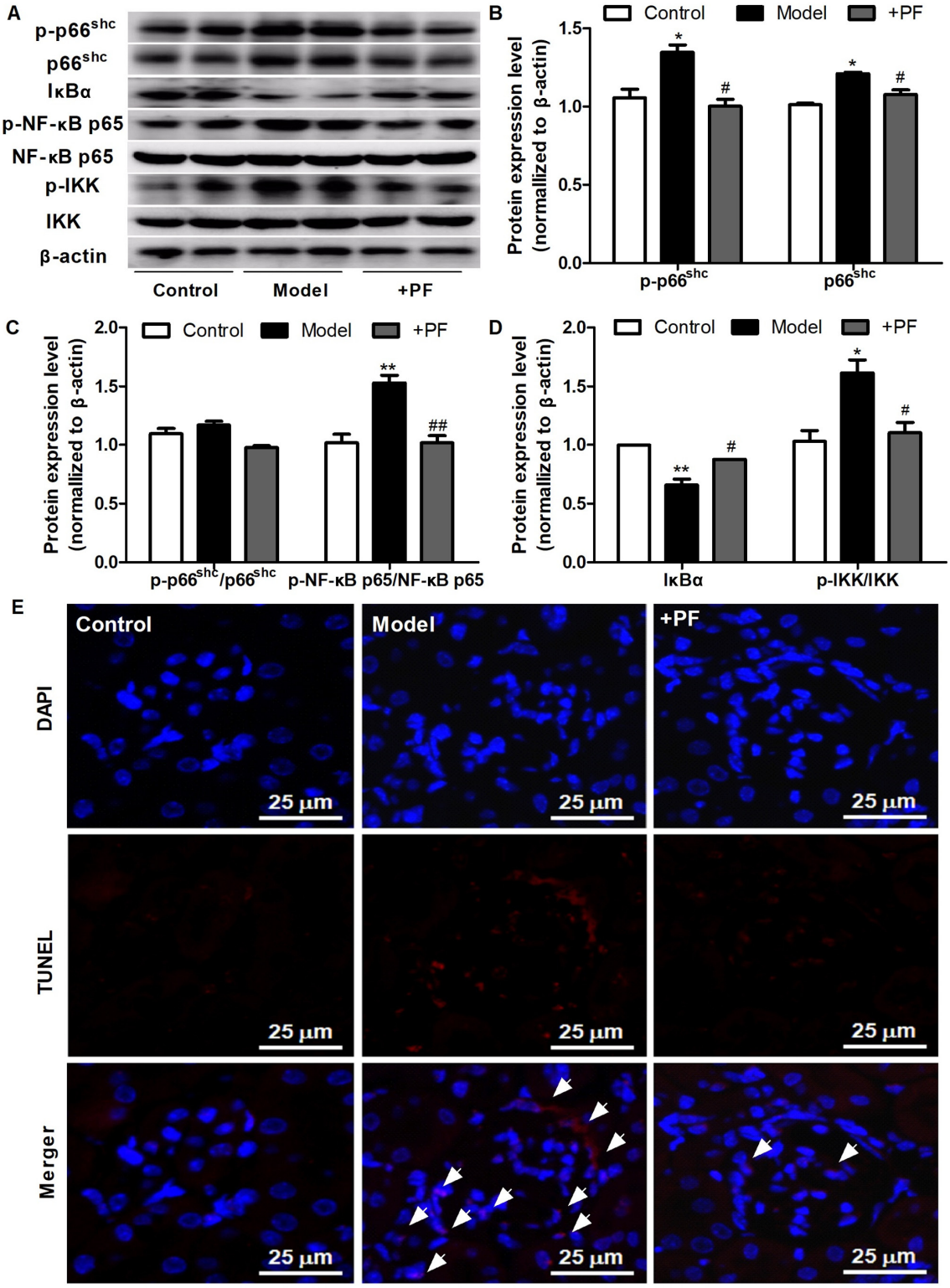

Figure 5. PF attenuates kidney injury in diabetic mice. (A) Western blot analysis of p-p66^{shc}, total p66^{shc}, IκBα, p-NF-κB p65, total NF-κB p65, p-IKKα/β, total IKKα/β and β-actin. (B) Densitometric analysis of p-p66^{shc} and total p66^{shc}. (C) Densitometric analyses of p-p66^{shc}/p66^{shc} and p-NF-κB p65/NF-κB p65. (D) Densitometric analyses of IκBα and p-IKKα/β/IKKα/β. (E) Representative image of the TUNEL staining; x400 magnification; white arrowheads indicate TUNEL-positive cells. Data are expressed as the mean ± SEM, n=3. *P<0.05, **P<0.01 vs. control group; $^{\#}$P<0.05, $^{\#\#}$P<0.01 vs. HG group. PF, piperazine ferulate; HG, high glucose; p-, phosphorylated; Shc, Src homology/collagen; +PF, diabetic nephropathy + PF.

identified that PF reversed glomerular fibrosis induced by hyperglycemia (Fig. 6F and G). These results suggested that PF reversed the HG-induced mesangial matrix expansion in the glomerulus.

Discussion

DN is the leading cause of end-stage renal failure, but the pathogenesis of DN is not yet fully understood. Persistent

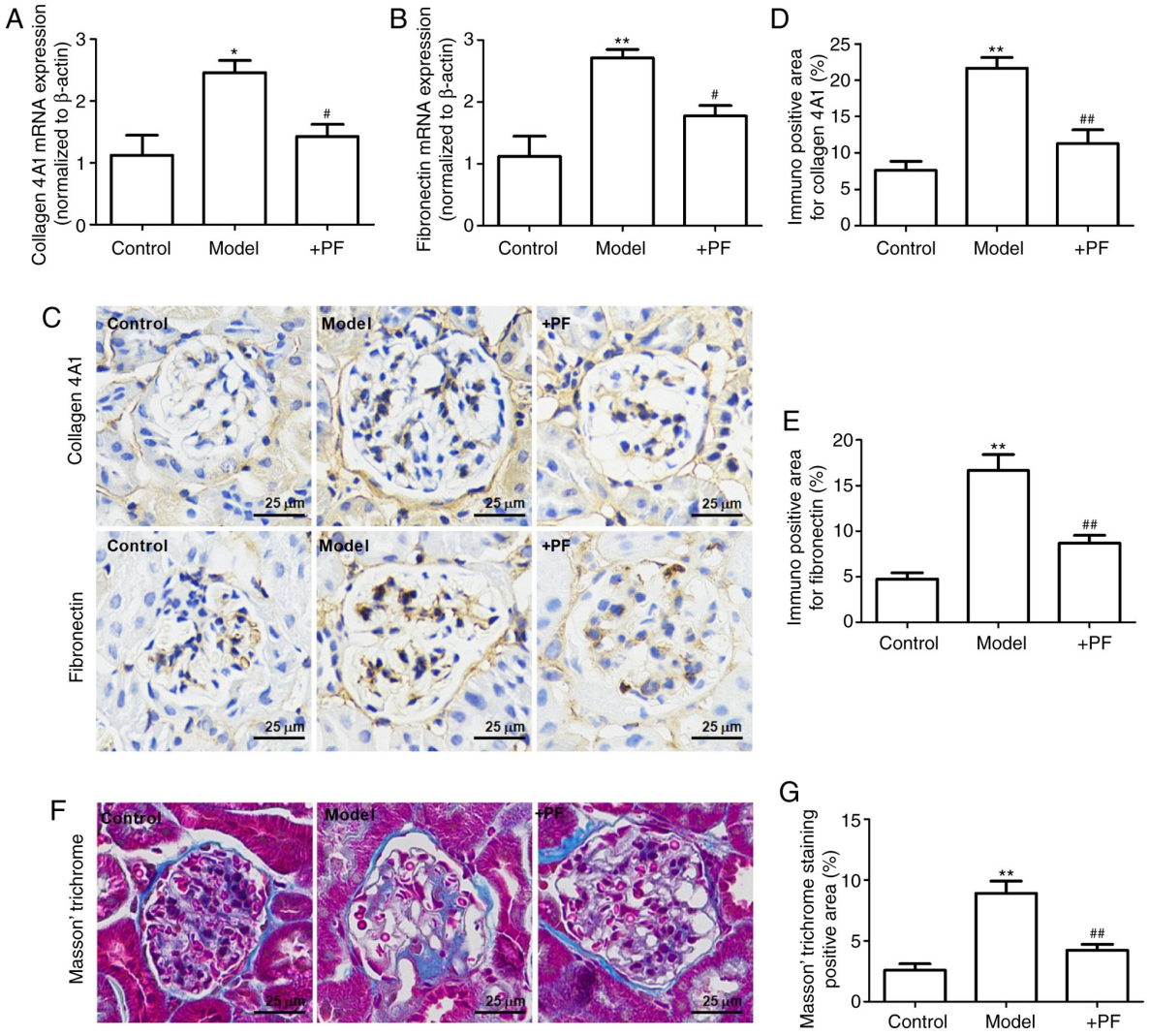

Figure 6. PF attenuates mesangial matrix expansion in diabetic mice. Effect of PF on the mRNA expression levels of (A) collagen 4A1 and (B) fibronectin. (C) Immunohistochemistry images of collagen 4A1 and fibronectin; x400 magnification. (D) Quantification analyses of immunohistochemistry staining of collagen 4A1. (E) Quantification analyses of immunohistochemistry staining of fibronectin. (F) Masson's trichrome staining; x400 magnification. (G) Quantification analyses of Masson's trichrome staining. Data are expressed as the mean ± SEM, n=3. *P<0.05, **P<0.01 vs. control group. $^{\#}$P<0.05, $^{\#\#}$P<0.01 vs. model group. PF, piperazine ferulate; +PF, diabetic nephropathy + PF.

hyperglycemia leads to increased glycation end products, oxidative stress, the production of inflammatory cytokines and hemodynamic abnormalities (29). These factors individually and/or synergistically result in the pathological features of DN, including the thickening of the glomerular basement membrane, damage to glomerular cells, mesangial matrix expansion and tubulointerstitial fibrosis (30). HG-induced damage to glomerular cells, including glomerular endothelial cells, podocytes and mesangial cells, is a key factor in exacerbating the progression of DN (11,30-32). Moreover, damage to glomerular endothelial cells and podocytes causes filtration barrier damage and accelerates the excretion of albuminuria (7,31). Mesangial cells maintain the structure and function of the glomerulus, and also regulate filter barrier function by controlling the capillary surface area (31). Therefore, preventing mesangial cell apoptosis is of utmost importance for the prevention and treatment of DN.

ROS serve a key role in glomerular mesangial cell apoptosis under hyperglycemic conditions (33). Some *in vivo* studies have reported that antioxidant compounds, such as N-acetylcysteine (34), folic acid (35) and carnosic acid (36), were able to delay the progression of DN by regulating the production of ROS. However, none of these compounds have been approved for clinical use as anti-diabetic nephropathy drugs. Therefore, the therapeutic targets of DN warrant further investigation.

$p66^{Shc}$ is predominantly located in the cytoplasm, with 10-40% located in the mitochondrial membrane space in a complex with the mitochondrial heat shock protein (37), and is involved in the apoptosis of mesangial cells under hyperglycemic conditions (17).

In China, PF is used in the treatment of various kidney diseases, and no severe adverse reactions have been reported to date. An acute toxicity test revealed that the median lethal dose of PF to Kunming mice was 3,580.1±251.7 mg/kg. Moreover, reproductive toxicity studies have reported that PF has no obvious embryonic side-effects and teratogenic effects (the data are from the package insert of PF) (38). In

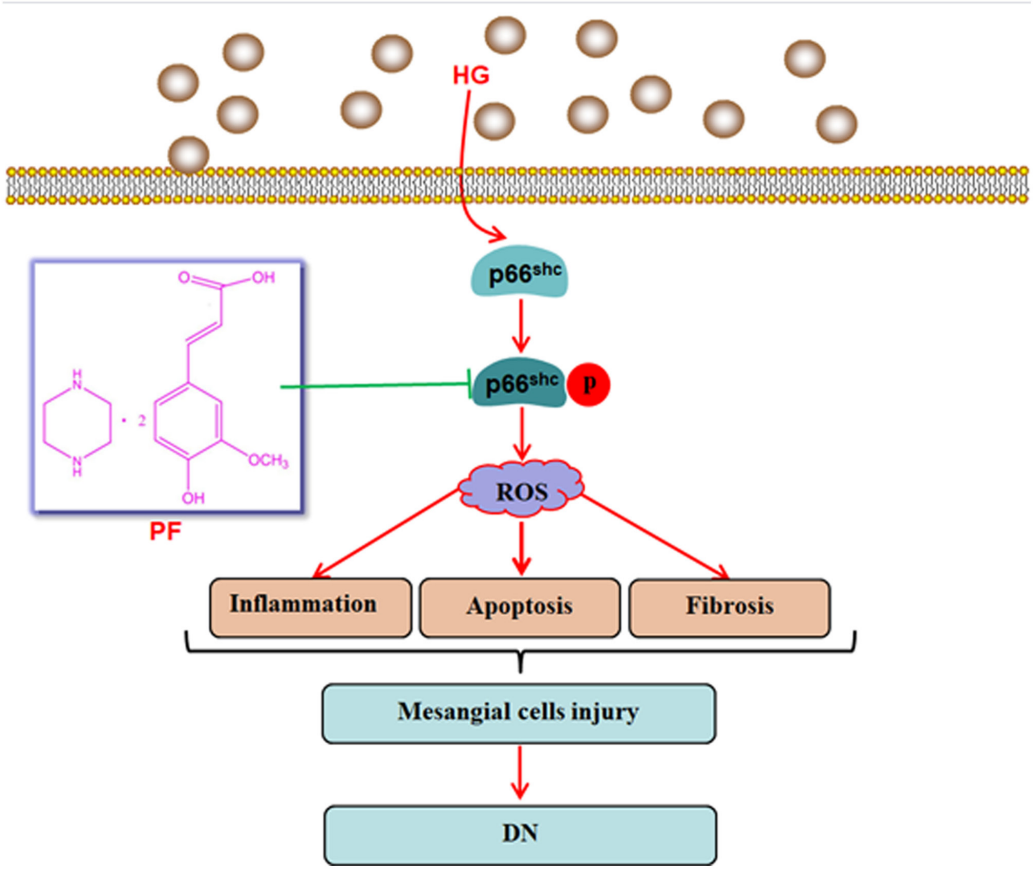

Figure 7. Schematic diagram of pathways involved in the protective effects of PF against HG-induced mesangial cell injury. In the diabetic environment, HG induces glomerular mesangial cell injury, which is characterized by an increase in apoptosis, inflammatory cytokine release and mesangial matrix synthesis. PF attenuated HG-induced mesangial cell injury by inhibiting $p66^{Shc}$. PF, piperazine ferulate; HG, high glucose; Shc, Src homology/collagen; ROS, reactive oxygen species; DN, diabetic nephropathy.

the present study, it was found that PF was an efficient drug against HG-induced mesangial cell injury by inhibiting $p66^{Shc}$. For example, PF decreased the levels of IL-6 and TNF-α, the generation of ROS and the nuclear translocation of NF-κB p65 in HG-treated mesangial cells. Furthermore, PF inhibited the HG-induced upregulation of fibronectin and collagen 4A1 expression levels in *in vitro* and *in vivo* experiments. It was also demonstrated that the multiple pharmacological functions of PF, including anti-inflammatory, anti-apoptotic and anti-fibrotic effects, were abolished when the mesangial cells overexpressed of $p66^{Shc}$. The phosphorylation of $p66^{Shc}$ is a critical step for the production of ROS, and both UV radiation and H_2O_2 can phosphorylate the serine residue of $p66^{Shc}$ (39). The present study identified that PF decreased the protein expression level of p-$p66^{Shc}$ in mesangial cells exposed to HG. However, the present study also has limitations. Although the study demonstrated that PF could inhibit the phosphorylation level of $p66^{Shc}$ in both *in vivo* and *in vitro* experiments, the mechanism by which PF inhibits the phosphorylation of $p66^{Shc}$ is not clear. Further studies are required to determine the mechanisms via which PF inhibits the phosphorylation of serine of $p66^{Shc}$ through molecular docking and molecular-protein interaction test.

In conclusion, the present study demonstrated that the inhibition of $p66^{Shc}$ activation may be used as a therapeutic approach to attenuate mesangial cells damage induced by hyperglycemia, and that PF attenuated HG-induced mesangial cell injury by inhibiting $p66^{Shc}$ (Fig. 7). The results provided a potential mechanism via which PF attenuates the development of DN, but further studies are warranted to evaluate the exact mechanisms underlying the regulatory effects of PF on $p66^{Shc}$.

Acknowledgements

Not applicable.

Funding

The present study was supported financially by the National Natural Science Foundation of China (grant no. 81603171), Hunan Provincial Natural Scientific Foundation (grant nos. 2018JJ3743 and 2020JJ5841), Scientific Research Project of Hunan Provincial Health Commission (grant nos. B2019157 and B2019158) and the Open Sharing Fund for the Large-scale Instruments of Central South University (grant no. CSUZC202055).

Availability of data and materials

All data generated or analyzed during the present study are included in this published article.

Authors' contributions

DXX, LYY and XDY designed the study. YYY and RRD performed the experiments. YYY and ZC analyzed the data. YYY wrote the manuscript, and revised the manuscript with XDY. YYY and RRD confirm the authenticity of all the raw data. All authors read and approved the final version of the manuscript.

Ethics approval and consent to participate

All experimental protocols were approved by the Ethics Committee of Animal Experiments of the Central South University, and were performed in accordance with the Guidelines for the Care and Use of Laboratory Animals.

Patient consent for publication

Not applicable.

Competing interests

The authors declare that they have no competing interests.

References

1. Mou X, Chenv JW, Zhou DY, Liu K, Chen LJ, Zhou D and Hu YB: A novel identified circular RNA, circ_0000491, aggravates the extracellular matrix of diabetic nephropathy glomerular mesangial cells through suppressing miR101b by targeting TGFbetaRI. Mol Med Rep 22: 3785-3794, 2020.
2. Cho NH, Shaw JE, Karuranga S, Huang Y, da Rocha Fernandes JD, Ohlrogge AW and Malanda B: IDF diabetes atlas: Global estimates of diabetes prevalence for 2017 and projections for 2045. Diabetes Res Clin Pract 138: 271-281, 2018.
3. Yang X, Hu C, Wang S and Chen Q: Clinical efficacy and safety of Chinese herbal medicine for the treatment of patients with early diabetic nephropathy: A protocol for systematic review and meta-analysis. Medicine (Baltimore) 99: e20678, 2020.
4. Jia Q, Yang R, Liu XF, Ma SF and Wang L: Genistein attenuates renal fibrosis in streptozotocin-induced diabetic rats. Mol Med Rep 19: 423-431, 2019.
5. Zhang J, Dong XJ, Ding MR, You CY, Lin X, Wang Y, Wu MJ, Xu GF and Wang GD: Resveratrol decreases high glucose induced apoptosis in renal tubular cells via suppressing endoplasmic reticulum stress. Mol Med Rep 22: 4367-4375, 2020.
6. Dou L and Jourde-Chiche N: Endothelial toxicity of high glucose and its by-products in diabetic kidney disease. Toxins (Basel) 11: 578, 2019.
7. Tung CW, Hsu YC, Shih YH, Chang PJ and Lin CL: Glomerular mesangial cell and podocyte injuries in diabetic nephropathy. Nephrology (Carlton) 23 (Suppl 4): S32-S37, 2018.
8. Chen X, Yang Y, Liu C, Chen Z and Wang D: Astragaloside IV ameliorates high glucoseinduced renal tubular epithelial mesenchymal transition by blocking mTORC1/p70S6K signaling in HK2 cells. Int J Mol Med 43: 709-716, 2019.
9. Maezawa Y, Cina D and Quaggin SE: Glomerular cell biology. Chapter 22. In: The Kidney. 5th edition. Alpern RJ, Moe OW and Caplan M (eds). San Diego. Academic Press, pp721-755., 2013
10. Mishra R, Emancipator SN, Kern T and Simonson MS: High glucose evokes an intrinsic proapoptotic signaling pathway in mesangial cells. Kidney Int 67: 82-93, 2005.
11. Tsai YC, Kuo MC, Hung WW, Wu LY, Wu PH, Chang WA, Kuo PL and Hsu YL: High glucose induces mesangial cell apoptosis through miR-15b-5p and promotes diabetic nephropathy by extracellular vesicle delivery. Mol Ther 28: 963-974, 2020.
12. Ostergaard JA, Cooper ME and Jandeleit-Dahm KAM: Targeting oxidative stress and anti-oxidant defence in diabetic kidney disease. J Nephrol 33: 917-929, 2020.
13. Di Lisa F, Giorgio M, Ferdinandy P and Schulz R: New aspects of p66Shc in ischaemia reperfusion injury and other cardiovascular diseases. Br J Pharmacol 174: 1690-1703, 2017.
14. Giorgio M, Migliaccio E, Orsini F, Paolucci D, Moroni M, Contursi C, Pelliccia G, Luzi L, Minucci S, Marcaccio M, *et al*: Electron transfer between cytochrome *c* and p66Shc generates reactive oxygen species that trigger mitochondrial apoptosis. Cell 122: 221-233, 2005.
15. Clark JS, Faisal A, Baliga R, Nagamine Y and Arany I: Cisplatin induces apoptosis through the ERK-p66shc pathway in renal proximal tubule cells. Cancer Lett 297: 165-170, 2010.
16. Miller B, Palygin O, Rufanova VA, Chong A, Lazar J, Jacob HJ, Mattson D, Roman RJ, Williams JM, Cowley AWJr, *et al*: p66Shc regulates renal vascular tone in hypertension-induced nephropathy. J Clin Invest 126: 2533-2546, 2016.
17. Menini S, Amadio L, Oddi G, Ricci C, Pesce C, Pugliese F, Giorgio M, Migliaccio E, Pelicci P, Iacobini C and Pugliese G: Deletion of p66Shc longevity gene protects against experimental diabetic glomerulopathy by preventing diabetes-induced oxidative stress. Diabetes 55: 1642-1650, 2006.
18. Zhan M, Usman I, Yu J, Ruan L, Bian X, Yang J, Yang S, Sun L and Kanwar YS: Perturbations in mitochondrial dynamics by p66Shc lead to renal tubular oxidative injury in human diabetic nephropathy. Clin Sci (Lond) 132: 1297-1314, 2018.
19. Jiang W, Xiao T, Han W, Xiong J, He T, Liu Y, Huang Y, Yang K, Bi X, Xu X, *et al*: Klotho inhibits PKCalpha/p66SHC-mediated podocyte injury in diabetic nephropathy. Mol Cell Endocrinol 494: 110490, 2019.
20. Li D, Li B, Peng LX, Liu R and Zeng N: Therapeutic efficacy of piperazine ferulate combined with irbesartan in diabetic nephropathy: A Systematic review and meta-analysis. Clin Ther 42: 2196-2212, 2020.
21. Liu Z, Pan J, Sun C, Zhou J and Li NA: Clinical effects of perazine ferulate tablets combined with eucalyptol limonene pinene enteric soft capsules for treatment of children with IgA nephropathy. Exp Ther Med 12: 169-172, 2016.
22. Zheng L, Chen S, Wang F, Huang S, Liu X, Yang X, Zhou H, Zhao GP, Luo M, Li S and Chen J: Distinct responses of gut microbiota to Jian-Pi-Yi-Shen decoction are associated with improved clinical outcomes in 5/6 nephrectomized rats. Front Pharmacol 11: 604, 2020.
23. Jianzhi S, Qizeng W, Bin L, Wenhui L, Yunpeng C, Chenrong F, Lin Z, Huiting C: Piperazine ferulate exerts antihypertensive effect and improves endothelial function in vitro and in vivo via the activation of endothelial nitric oxide synthase. Cell Mol Biol (Noisy-le-grand) 65: 119-124, 2019.
24. Yang YY, Shi LX, Li JH, Yao LY and Xiang DX: Piperazine ferulate ameliorates the development of diabetic nephropathy by regulating endothelial nitric oxide synthase. Mol Med Rep 19: 2245-2253, 2019.
25. Livak KJ and Schmittgen TD: Analysis of relative gene expression data using real-time quantitative PCR and the 2(-Delta Delta C(T)) method. Methods 25: 402-408, 2001.
26. Wong YH and Abdul Kadir H: Induction of mitochondria-mediated apoptosis in Ca Ski human cervical cancer cells triggered by mollic acid arabinoside isolated from leea indica. Evid Based Complement Alternat Med 2012: 684740, 2012.
27. Cheng YS, Chao J, Chen C, Lv LL, Han YC and Liu BC: The PKCβ-p66shc-NADPH oxidase pathway plays a crucial role in diabetic nephropathy. J Pharm Pharmacol 71: 338-347, 2019.
28. Haller M, Khalid S, Kremser L, Fresser F, Furlan T, Hermann M, Guenther J, Drasche A, Leitges M, Giorgio M, *et al*: Novel Insights into the PKCbeta-dependent Regulation of the Oxidoreductase p66Shc. J Biol Chem 291: 23557-23568, 2016.
29. Dragos D, Manea MM, Timofte D and Ionescu D: Mechanisms of herbal nephroprotection in diabetes mellitus. J Diabetes Res 2020: 5710513, 2020.
30. Rayego-Mateos S, Morgado-Pascual JL, Opazo-Rios L, Guerrero-Hue M, Garcia-Caballero C, Vazquez-Carballo C, Mas S, Sanz AB, Herencia C, Mezzano S, *et al*: Pathogenic pathways and therapeutic approaches targeting inflammation in diabetic nephropathy. Int J Mol Sci 21: 3798, 2020.
31. Davidson A, Berthier C and Kretzler M. Pathogenetic Mechanisms in lupus nephritis. Chapter 18. In: Dubois' Lupus Erythematosus and Related Syndromes. 8th edition. Wallace DJ and Hahn BH (eds). W.B. Saunders, Philadelphia, PA, pp237-255, 2013.
32. Fu J, Wei C, Zhang W, Schlondorff D, Wu J, Cai M, He W, Baron MH, Chuang PY, Liu Z, *et al*: Gene expression profiles of glomerular endothelial cells support their role in the glomerulopathy of diabetic mice. Kidney Int 94: 326-345, 2018.
33. Wan C, Su H and Zhang C: Role of NADPH oxidase in metabolic disease-related renal injury: An update. Oxid Med Cell Longev 2016: 7813072, 2016.

34. Chen X and Fang M: Oxidative stress mediated mitochondrial damage plays roles in pathogenesis of diabetic nephropathy rat. Eur Rev Med Pharmacol Sci 22: 5248-5254, 2018.
35. Ebaid H, Bashandy SAE, Abdel-Mageed AM, Al-Tamimi J, Hassan I and Alhazza IM: Folic acid and melatonin mitigate diabetic nephropathy in rats via inhibition of oxidative stress. Nutr Metab (Lond) 17: 6, 2020.
36. Xie Z, Zhong L, Wu Y, Wan X, Yang H, Xu X and Li P: Carnosic acid improves diabetic nephropathy by activating Nrf2/ARE and inhibition of NF-κB pathway. Phytomedicine 47: 161-173, 2018.
37. Orsini F, Migliaccio E, Moroni M, Contursi C, Raker VA, Piccini D, Martin-Padura I, Pelliccia G, Trinei M, Bono M, *et al*: The life span determinant p66Shc localizes to mitochondria where it associates with mitochondrial heat shock protein 70 and regulates trans-membrane potential. J Biol Chem 279: 25689-25695, 2004.
38. DRUGDATAEXPY. 2009. Chongqing. http://zy.yaozh.com/instruct/20160513-1/35.jpg. Accessed March 1, 2021.
39. Nemoto S and Finkel T: Redox regulation of forkhead proteins through a p66shc-dependent signaling pathway. Science 295: 2450-2452, 2002.